We are IntechOpen, the world's leading publisher of Open Access books
Built by scientists, for scientists

6,900
Open access books available

185,000
International authors and editors

200M
Downloads

154
Countries delivered to

Our authors are among the

TOP 1%
most cited scientists

12.2%
Contributors from top 500 universities

CLARIVATE ANALYTICS
BOOK CITATION INDEX
INDEXED

WEB OF SCIENCE™

Selection of our books indexed in the Book Citation Index
in Web of Science™ Core Collection (BKCI)

Interested in publishing with us?
Contact book.department@intechopen.com

Optimum Design of End-Pumped Solid-State Lasers

Gholamreza Shayeganrad
Institute of Photonics Technologies, Department of Electrical Engineering,
National Tsinghua University,
Taiwan

1. Introduction

The principle of laser action was first experimentally demonstrated in 1960 by T. Maiman (Maiman, 1960). This first system was a solid-state laser in which a ruby crystal and a flashlamp served as gain medium and pump source, respectively. Soon after this first laser experiment, it was realized that solid-state lasers are highly attractive sources for various scientific and industrial applications such as laser marking, material processing, holography, spectroscopy, remote sensing, lidar, optical nonlinear frequency conversion, THz frequency generation (Koechner, 2006; Hering et al., 2003; Ferguson & Zhang, 2003; Sennaroghlu, 2007). Since the early 1980's with the development of reliable high power laser diode and the replacement of traditional flashlamp pumping by laser-diode pumping, the diode-pumped solid-state lasers, DPSSL's, have received much attention and shown the significant improvements of laser performance such as optical efficiency, output power, frequency stability, operational lifetime, linewidth, and spatial beam quality.

Nd:YAG and Nd:YVO$_4$ crystals have been extensively used as a gain medium in commercial laser products with high efficiency and good beam quality. The active ion of Nd^{3+} has three main transitions of $^4F_{3/2} \rightarrow ^4I_{9/2}$, $^4F_{3/2} \rightarrow ^4I_{11/2}$, and $^4F_{3/2} \rightarrow ^4I_{13/2}$ with the respective emission lines of 0.94, 1.06 and 1.3 μm. The emission wavelengths of DPSSL's associated with nonlinear crystals cover a wide spectral region from ultraviolet to the mid-infrared range and very often terahertz range by difference frequency mixing process in simultaneous multi-wavelength solid-state lasers (Saha et al., 2006; Guo etal., 2010).

DPSSL's are conventionally categorized as being either end-pumped or side pumped lasers. End-pumping configuration is very popular because of higher efficiency, excellent transverse beam quality, compactness, and output stability which make it more useful for pumping tunable dye and Ti: Sapphire laser, optical parametric oscillator/amplifier, and Raman gain medium. The better beam quality is due to the high degree of spatial overlap between pump and laser modes while the high efficiency is dependent on good spatial mode-matching between the volume of pump and laser modes or nondissipating of pump energy over pumping regions that are not used by laser mode. In addition, end pumping allows the possibility of pumping a thin gain medium such as disk, slab, and microchip lasers that are not be accessed from the side-pumping (Fan &. Byer, 1998; Alfrey, 1989; Carkson & Hanna,1988; Sipes, 1985; Berger et al. 1987).

The side-pumping geometry allows scaling to high-power operation by increasing the number of pump sources placed around the gain medium before occurring thermal fracture. In this arrangement the pump power is uniformly distributed and absorbed over a large volume of the crystal which leads to reduce the thermal effects such as thermal lensing and thermal induced stress. However, the power scaling of end-pumped lasers is limited due to the physically couple of many diode-lasers into a small pumped volume and the thermal distortion inside the laser crystal. To improve power scaling of an end-pumped laser, a fiber-coupled laser-diode array with circular beam profile and high-output power and a crystal with better thermal properties can be employed as a pump source and gain medium, respectively (Hemmeti & Lesh, 1994; Fan & Sanchez, 1989; Mukhopadhyay, 2003; Hanson, 1995; Weber, 1998; Zhuo, 2007; Sulc, 2002; MacDonald, 2000).

Laser performance is characterized by threshold and slope efficiency. The influence of pump and laser mode sizes on the laser threshold and slope efficiency has been well investigated (Hall et al. 1980; Hall, 1981; Risk, 1988; Laporta &. Brussard, 1991; Fan & Sanchez, 1990; Clarkson & Hanna, 1989; Xiea et al., 1999). It is known a smaller value of the pump radius leads to a lower threshold and a higher slope efficiency. However, in the case of fiber-coupled end-pumped lasers, due to pump beam quality, finite transverse dimension, diffraction, absorption and finite length of the gain medium, the pump size can be decreased only to a certain value.

It is worthwhile to mention, that for both longitudinal and transverse pumping, the pump radius varies within the crystal mainly because of absorption and diffraction. It is possible to consider a constant pump radius within the crystal when the crystal length is much smaller than the Rayleigh range of the pump beam and also than the focal length of thermal lens. However, in the case of longitudinal pumping, the pump intensity is still a function of distance from the input end even this circumstance is also satisfied. Meanwhile, the lower brightness of the laser-diodes than the laser beam makes the Rayleigh distance of the pump beam considerably be shorter than the crystal length.

The effect of pump beam quality on the laser threshold and slope efficiency of fiber-coupled end-pumped lasers has been previously investigated (Chen et al., 1996, 1997). The model is developed based on the space-dependent rate-equations and the approximations of paraxial propagation on pump beam and gain medium length much larger than absorption length. Further development was made by removing the approximation on gain medium length (Chen, 1999), while for a complete description, rigorous analysis is required.

In this chapter, we initially reviewed the space-dependent rate equation for an ideal four-level end-pumped laser. Based on the space-dependent rate equation and minimized root-mean-square of pump beam radius within the gain medium, a more comprehensive and accurate analytical model for optimal design an end-pumped solid-state laser has been presented. The root-mean-square of the pump radius is developed generally by taking a circular–symmetric Gaussian pump beam including the M^2 factor. It is dependent on pump beam properties (waist location, M^2 factor, waist radius, Rayleigh range) and gain medium characteristics (absorption coefficient at pump wavelength and gain medium length). The optimum mode-matching is imposed by minimizing the root-mean-square of pump beam radius within the crystal. Under this condition, the optimum design key parameters of the optical coupling system have been analytically derived. Using these parameters and the

linear approximate relation of output power versus input power, the parameters for optimum design of laser cavity are also derived. The requirements on the pump beam to achieve the desired gain at the optimum condition of mode-matching are also investigated. Since thermal effects are the final limit for scaling end-pumped solid-state lasers, a relation for thermal focal length at this condition is developed as a function of pump power, pump beam M^2 factor, and physical and thermal-optics of gain medium properties. The present model provides a straightforward procedure to design the optimum laser resonator and the optical coupling system.

2. Space-dependent rate equation

The rate equation is a common approach for dynamically analyzing the performance of a laser. For a more accurate analysis of characteristics of an end-pumped laser, particularly the influence of the pump to laser mode sizes, it is desirable to consider the spatial distribution of inversion density and the pump and laser modes in the rate equation. The space-dependent rate equation based on single mode operation for an ideal four level laser is developed by Laporta and. Brussard (Laporta &. Brussard, 1991):

$$\frac{dN(x,y,z)}{dt} = R(x,y,z) - \sigma_e c_0 \frac{S(x,y,z)}{h\nu_l} N(x,y,z) - \frac{N(x,y,z)}{\tau} \tag{1}$$

$$\frac{dq}{dt} = \sigma_e c_0 \iiint \frac{S(x,y,z)}{h\nu_l} N(x,y,z) dV - \frac{q}{\tau_c} \tag{2}$$

where z is the propagating direction, N is the upper energy level population density, R is the total pumping rate into the upper level per unit volume, S is the cavity mode energy density, σ_e is the cross section of laser transition, c_0 is the light velocity in the vacuum, h is the Plank's constant, ν_l is the frequency of the laser photon , q is the total number of photons in the cavity mode, τ is the upper-level life-time, and τ_c is the photon lifetime. In Eq. (2) the integral is calculated over the entire volume of the active medium. The photon lifetime can be expressed as $\tau_c = 2l_e/\delta c_0$, where $l_e = l_{ca} + (n-1)l$ is the effective length of the resonator, n is refractive index of the active material, l_{ca} and l are the geometrical length of the resonator and the active medium, respectively, and $\delta = 2\alpha_i l - \ln(R_1 R_2) + \delta_c + \delta_d \approx 2\delta_i + T + \delta_c + \delta_d$ is the total logarithmic round-trip cavity-loss of the fundamental intensity, T is the power transmission of the output coupler, δ_i represents the loss proportional to the gain medium length per pass such as impurity absorption and bulk scattering, δ_c is the non-diffraction internal loss such as scattering at interfaces and Fresnel reflections, and δ_d is the diffraction losses due to thermally induced spherical aberration. The approximation is valid for the small values of T.

Note that to write Eq. (2) the assumption of a small difference between gain and logarithmic loss has been assumed which maintains when intracavity intensity is a weak function of z. For a continuous-wave (CW) laser this situation always holds while for a pulsed laser, it is valid only when the laser is not driven far above the threshold. It follows that this analysis is appropriated to describe the behavior of low gain diode-pumped lasers, but is not adequate for gain-switched or Q-switched lasers and in general for high gain lasers. It is also assumed that the transverse mode profile considered for the unloaded resonator is not substantially modified by the optical material inside the cavity.

The pumping rate R can be related to the input pump power P_{in}

$$\iiint R(x,y,z)dV = \eta_p \frac{P_{in}}{h\nu_l} \tag{3}$$

where $\eta_p = \eta_t\eta_a(\nu_l/\nu_p)$ is the pumping efficiency, η_t is the optical transfer efficiency (ratio between optical power incident on the active medium and that of emitted by the pump source), and $\eta_a \approx 1-exp(-al)$ is the absorption efficiency (ratio between power absorbed in the active medium and that of entering the gain medium), α is the absorption coefficient at pump wavelength, l is the crystal length, ν_p is the frequency of the pump photon, and the integral extends again over the volume of the active material. Under the stationary condition, a relationship between the energy density in the cavity and the pumping rate can be easily derived. We define a normalized pump distribution within the gain medium as

$$r_p(x,y,z) = \frac{R(x,y,z)}{R_0} \tag{4}$$

where $\iiint r_p(x,y,z)dV = 1$ and R_0 represents therefore the total number of photons absorbed per unit time in the active medium. We also define a normalized mode distribution as

$$s_l(x,y,z) = \frac{S(x,y,z)}{S_0} \tag{5}$$

where $\int_1 ns_l(x,y,z)dV + \int_2 s_l(x,y,z)dV = 1$, and S_0 is the total energy of cavity mode corresponding to the total number of photons $q=S_0/h\nu_l$ The first integral is taken over the whole field distribution in the region of the active medium and the second in the remaining volume of the resonator.

Substituting Eq. (1) into (2), and considering Eqs. (3)-(5), under the steady-state condition, we have

$$P_{in} = \frac{\delta h\nu_l}{2\eta_p l_e \sigma_e \tau} \left[\iiint \frac{s_l(x,y,z)r_p(x,y,z)}{c_0 S_0 s_l(x,y,z)/I_{sat}+1} dV \right]^{-1} \tag{6}$$

where $I_{sat}= h\nu_l/\sigma_e\tau$ is the saturation intensity. In the threshold limit ($S_0\approx0$) we obtain the following formula for the threshold pump power:

$$P_{th} = \frac{\delta\; h\nu_l}{2\sigma_e\tau\eta_p l_e} V_{eff} \tag{7}$$

where

$$V_{eff} = \left[\iiint s_l(x,y,z).r_p(x,y,z)dV \right]^{-1} \tag{8}$$

introduces the effective volume of spatial overlap between pump and cavity modes.

In the approximation of intracavity intensity much less than saturation intensity, the argument of the integral in (6) can be expanded around zero based on Taylor series and keep the first term as

$$\frac{s_l r_p}{c_0 S_0 s_l / I_{sat} + 1} \cong \left(1 - c_0 S_0 s_l / I_{sat}\right) s_l r_p \tag{9}$$

Inserting Eq. (9) into Eq. (6) and developing the integral with assuming the plane wave approximation, $c_0 S_0 / l_e = 2P$, where $P = P_{out}/T$ is the intracavity power of one of the two circulating waves in the resonator, yields

$$P_{out} = \eta_s \left[P_{in} - P_{th}\right] \tag{10}$$

where

$$\eta_s = \frac{T}{\delta} \eta_p V_{slope} \tag{11}$$

is the slope efficiency and

$$V_{slope} = \frac{\left(\iiint s_l(x,y,z).r_p(x,y,z)dV\right)^2}{\iiint s_l^2(x,y,z).r_p(x,y,z)dV} \tag{12}$$

represents the mode-matching efficiency. The slope efficiency η_s can be defined as the product of the pumping efficiency η_p, the output coupling efficiency $\eta_c = T/\delta$, and the spatial overlap efficiency V_{slope}. The slope efficiency measures the increase of the output power as the pump power increases. It is generally somewhat larger than the total power conversion efficiency. For high slope efficiency, one wants high η_p, and low δ. It can also be achieved by increasing T if other losses are not low, but this is undesirable because it increases threshold pump power.

We should note that for mode-to-pump size ratio greater than unity, the linear approximation in Eq. (10) is valid also when the intracavity intensity is comparable with the saturation intensity. It should be also noted that for simplicity we have considered the plane wave approximation, but the formalism can be easily expanded for non-plane wave, such as a Gaussian beam profile.

From Eq. (7), threshold pump power depends linearly on the effective mode volume, and inversely on the product of the effective stimulated-emission cross-section and the lifetime of laser transition. Thus, if laser transition lifetime be the only variable, it seems the longer lifetime results in a lower pump threshold for CW laser operation. However, the stimulated-emission cross section is also inversely proportional to the lifetime of laser transition. Offsetting this is the relation between the laser transition lifetime and the stimulated emission cross-section. In many instances, the product of these two factors is approximately constant for a particular active ion. Consequently, threshold is roughly and inversely proportional to the product of the effective stimulated emission cross-section and the lifetime of the laser transition. Notice that larger stimulated-emission cross section is useful

in a lower pump threshold for CW laser operation and a smaller cross section has advantages in Q-switch operation. On the other hand, slope efficiency depends on the overlap or mode-matching efficiency and losses as well. Overlap efficiency is dependent on the particular laser design but generally it is easier to achieve when laser pumping is used rather than flashlamp pumping.

The total round-trip internal loss, $L_i=2\delta_i+\delta_c+\delta_d$, in the system can be determined experimentally by the Findlay-Clay analysis. This was done by measuring the different pumping input power at the threshold versus the transmission of output coupling mirror as (Findlay & Clay 1966)

$$T = K_p P_{th} - L_i \tag{13}$$

where $K_p=(2\eta_p l_e/I_{sat}V_{eff})$ is the pumping coefficient.

According to Koechner (Koechner, 2006) the optimum output coupler transmission T_{opt} can be calculated using the following standard formula:

$$T_{opt} = (\sqrt{g_0 l_e / L_i} - 1)L_i \tag{14}$$

where g_0 is the small signal round-trip gain coefficient. The small-signal round-trip gain coefficient for an ideal four-level end-pumped laser is often expressed as:

$$g_0 = 2\sigma_e \iiint s_l(x,y,z)N(x,y,z)dV \tag{15}$$

According to Eqs. (1), (2) and (15), the small-signal round-trip gain coefficient which under the steady-state condition can be found as

$$g_0 = \frac{2\eta_p}{I_{sat}V_{eff}}P_{in} \tag{16}$$

As can be seen in (16), for an ideal four-level laser, the small-signal gain coefficient g_0 varies linearly with pump power and inversely with effective mode volume.

3. Optimum pumping system

A common configuration of a fiber-coupled laser diode end-pumped laser is shown in Fig. 1. In this arrangement, the coupled pump energy from a laser-diode into a fiber is strongly focused by a lens onto the gain medium. The w_{po} and w_{l0} are the pump and beam waists, respectively, l is the gain medium length, and z_0 is the location of pump beam waist.

Assuming a single transverse Gaussian fundamental mode (TEM$_{00}$) propagates in the cavity and neglecting from diffraction over the length of the gain medium, s_l can be expressed as:

$$s_l(x,y,z) = \frac{2}{\pi w_l^2(z)l_e}\exp\left(-2\frac{x^2+y^2}{w_l^2(z)}\right) \tag{17}$$
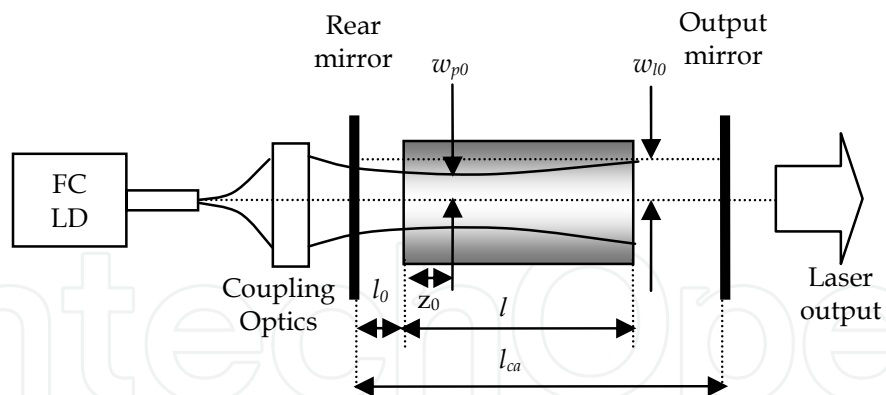
where

Fig. 1. Schematic diagram of a fiber-coupled laser-diode (FC LD) end-pumped solid-state laser.

$$w_l^2(z) = w_{l0}^2 \left[1 + \left(\frac{z\lambda_l}{n\pi w_{l0}^2} \right)^2 \right] \approx w_{l0}^2 \qquad (18)$$

represents the spot size at a distance z, where w_{l0} is the waist of the Gaussian beam, n is the refraction index of the crystal, λ_l is the fundamental laser wavelength in free space. The neglect of diffraction is justified if $n\pi w_{l0}^2 / \lambda_l$ is much larger than physical length l of the gain medium.

The intensity of the output beam comes out from a fiber-coupled laser-diode, r_p, may be described by a circular Gaussian function (Gong et al., 2008; Mukhopadhyay, 2003)

$$r_p(x,y,z) = \frac{2\alpha}{\pi w_p^2(z)[1 - \exp(-\alpha l)]} \exp\left(-2\frac{x^2 + y^2}{w_p^2(z)} - \alpha z \right) \qquad (19)$$

Here, α is the absorption coefficient at pump wavelength, l is the gain medium length, and $w_p(z)$ is the pump beam spot size given by:

$$w_p^2(z) = w_{p0}^2 \left[1 + \left(\frac{z - z_0}{z_R} \right)^2 \right] \qquad (20)$$

where w_{p0} is the waist of the pump beam, $z=z_0$ is the beam waist location and z_R is the Rayleigh range:

$$z_R = \frac{n\pi w_{p0}^2}{\lambda_p M^2} \qquad (21)$$

Note in the above equations $z = 0$ is taken at the incidence surface of the gain medium. In Eq. (21) M^2 is the times diffraction limited factor which indicates how close a laser is to being a single TEM$_{00}$ beam. An increasing value of M^2 represents a mode structure with more and more transversal modes. Beam M^2 factor is a key parameter which defines also how small a spot of a laser can be focused and the ability of the laser to propagate as a narrow thereby in some literatures it is called beam focusability factor. An important related quantity is the

confocal parameter or depth of focus of the Gaussian beam b=2z_R. It is a measure of the longitudinal extent of the focal region of the Gaussian beam or the distance that the Gaussian beams remains well collimated. In other word, over the focal region, the laser field, called the near field, stays roughly constant with a radius varying from w_{p0} to $\sqrt{2}$ w_{p0}. We see from (21), Rayleigh range is directly proportional to the beam waist w_{p0} and inversely proportional to the pump wavelength λ_P. Thus, when a beam is focused to a small spot size, the confocal beam parameter is short and the focal plane must be located with greater accuracy. A small spot size and a long depth of focus cannot be obtained simultaneously unless the wavelength of the light is short.

Inherent property of the laser beam is the relationship between beam waist w_0, far-field angle θ, and the index of refraction n. Based on the brightness theorem (Born & Wolf, 1999)

$$n\theta w_0 = C \geq M^2 \lambda_p / \pi \tag{22}$$

where C is a conserved parameter during focusing associated to the beam quality. For a fiber-coupled laser-diode, the value of C can simply be calculated from the product of fiber core radius and beam divergence angle. From Eq. (22), focusing a laser beam to a small spot size increases the beam divergence to reduce the intensity outside the Rayleigh range.

Putting Eqs. (17) and (19) into Eqs. (7) and (11), we obtain

$$P_{th} = \frac{\pi \delta w_{l0}^2 I_{sat}}{2\eta_p F(\alpha, l, w_{l0}, w_{p0}, z_0, z_R)} \tag{23}$$

$$\eta_s = \frac{T\eta_p}{\delta} \frac{F(\alpha, l, w_{l0}, w_{p0}, z_0, z_R)^2}{F(\alpha, l, w_{l0} / \sqrt{2}, w_{p0}, z_0, z_R)} \tag{24}$$

where

$$F(\alpha, l, \omega_{l0}, \omega_{p0}, z_0, z_R) = \frac{1}{1 - \exp(-\alpha l)} \times \int_0^l \frac{\alpha w_{l0}^2 \exp(-\alpha z)}{w_{l0}^2 + w_{p0}^2[1 + (z - z_0)^2 / z_R^2]} dz \tag{25}$$

is the mode-matching function describes the spatial-overlap of pump beam and resonator mode. The maximum value of the mode-matching function leads to the lowest threshold and the highest slope efficiency (Laporta & Brussard, 1991; Fan & Sanchez, 1990). Thereby the mode-matching function is the most important parameter to improve the laser performance. In general, this function cannot be solved analytically and to obtain the optimum pump focusing, Eq. (25) should be numerically solved. A closed form solution can be found by defining a suitable average pump spot size inside the active medium:

$$F(\alpha, l, \omega_{l0}, \omega_{p0}, z_0, z_R) = \frac{1}{1 - \exp(-\alpha l)} \times \int_0^l \frac{\alpha w_{l0}^2 \exp(-\alpha z)}{w_{l0}^2 + w_p^2(z)} dz = \frac{w_{l0}^2}{w_{l0}^2 + w_{p,rms}^2} \tag{26}$$

In this equation, $w_{p,rms}$ is the root-mean-square (RMS) of pump beam spot size within the active medium:

$$w_{p,rms} = \sqrt{\overline{w_p^2(z)}} \qquad (27)$$

where $\overline{w_p^2(z)}$ is the mean of square pump beam spot size along the active medium given by (Shayeganrad & Mashhadi, 2008):

$$\overline{w_p^2(z)} = \frac{\int_0^l w_p^2(z)\exp(-\alpha z)dz}{\int_0^l \exp(-\alpha z)dz} \qquad (28)$$

The exp(-αz) is the weighting function comes from the absorption of the pump beam along z direction. After putting Eq. (20) into Eq. (28) and performing the integrations we can obtain:

$$\overline{w_p^2(z)} = w_{p0}^2\left(1 + \frac{Z_0^2 - 2Z_0 f(L) + 2 - L(L+2)/[\exp(L)-1]}{Z_R^2}\right) \qquad (29)$$

where $Z_0 = az_0$, $Z_R = az_R$, and $L = \alpha l$ are dimensionless waist location, Rayleigh range and crystal length, respectively. In Eq. (29) $f(L) = 1 - \exp(-L)L/L_{eff}$ where $L_{eff} = 1 - \exp(-L)$ is the dimensionless parameter which defines the effective interaction length. Note that $L_{eff} \to L$ for L<<1, and $l_{eff} \to 1$ for L>>1. Thus for a strongly absorbing optical material (l>>1/α) the effective interaction length is much shorter than physical length of the medium. This configuration can be useful for designing the disk or microchip laser with high absorption coefficient and short length gain medium.

We see from (26) that the maximum value of mode-matching can be raised by minimizing the RMS of beam spot size at a constant mode size. A minimum value of $w_{p,rms}$ can occur when $\partial w_{p,rms}/\partial Z_0$ is equal to zero at a fixed L, w_{p0} and Z_R. The solution is

$$Z_{0,opt} = f(L) \Rightarrow L/2 \qquad (30)$$

After substituting Eq. (30) into (29) we obtain

$$\overline{w_{p,rms}^2}(z) = w_{p0}^2\left(1 + \frac{g^2(L)}{Z_R^2}\right) = \beta\left(Z_R + \frac{g^2(L)}{Z_R}\right) \qquad (31)$$

where $\beta = C/n\alpha$ is pump beam quality which is often quoted in square millimeter and $g^2(L) = 1 - \exp(-L)\left(L/L_{eff}\right)^2$. The value of parameter β can be calculated by substituting the value of C and the properties of the active medium, n, and α.

Differentiating (31) respect to Z_R and put it equal to zero, we find

$$Z_{R,opt} = g(L) \Rightarrow L/2\sqrt{3} \qquad (32)$$

In each expression the last form gives the asymptotic value for small L compared to unity. One sees that asymptotically the optimum waist location and Rayleigh range depend only on crystal length. While in the case of L>>1 or strong absorbing gain medium, they both tend to absorption lenght 1/α and are much shorter than physical length of the gain medium.

Fig. (2) shows the dimensionless optimum waist location and Rayleigh range of the pump beam. We can see, when absorption coefficient α increases, the optimum waist location and optimum Rayleigh range move closer to the incident surface of the active medium and they both increase with increasing active medium length l at a fixed α. These results were expected; because for large value of α, the pump beam is absorbed in a short length of the active medium. It can be also seen that the optimum waist location is larger than optimum Rayleigh range for 1<L<8 and for large L (L≥8) they both tend to the absorption length 1/α. For L=1.89 and L=1.26 optimum Rayleigh range and optimum waist location are equal to half of the absorption length independently on the gain medium length that is considered as the optimum range in several papers (Laporta & Brussard, 1991; Berger et al., 1987).
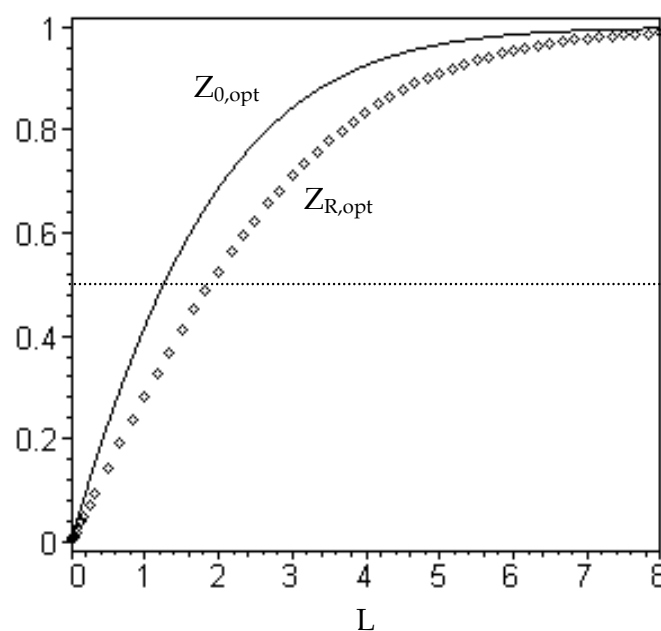
Fig. 2. The optimum dimensionless waist location and Rayleigh rang of the pump beam as a function of L.

Substitution (32) into (21) gives

$$w_{p0,opt} = \sqrt{\beta g(L)} \Rightarrow \sqrt{\beta L / 2\sqrt{3}} \tag{33}$$

Hence $w_{p,opt}$ becomes, after replacing Z_R by its value $g(L)$ into Eq. (31):

$$w_{p,opt} = \sqrt{2\beta g(L)} \tag{34}$$

From this equation, minimum pump spot size is a function of M^2 factor and two characteristic lengths: crystal length and absorption length 1/α. For $L \ll 1$, the minimum pump beam spot size $w_{p,opt}$ can be expressed in the following form:

$$w_{p,opt} \approx \sqrt{\beta L / \sqrt{3}} \tag{35}$$

As a result, optimum mode-matching function depends on the pump beam quality and gain medium characteristics as well. In practice, the experimentally measured optimum pump beam spot size $w_{p,opt}$, usually differs from that of calculated based on Eq. (34) because of the diffraction and thermal effects in a realistic laser gain medium. Nevertheless, this formula can provide a very good estimate for the $w_{p,opt}$.

Putting Eq. (34) into (22), optimum far-field-angle of pump beam is given by:

$$\theta_{p,opt} = \alpha \sqrt{\frac{\beta}{g(L)}} \tag{36}$$

It can be seen from Eqs. (34) and (36), optimum pump spot size and optimum pump beam divergence angle increase with increasing β to obtain maximum mode-matching efficiency. Equations (30), (33) and (36) provide a good guideline to design an optimum optical-coupling system. Again, these parameters are governed by the absorption coefficient, the gain medium length and the pump beam M^2 factor.

To reach the optimal-coupling, the incident Gaussian beam should be fitted to the aperture of the focusing lens with the largest possible extent without severe loss of pump power due to the finite aperture of the focusing lens and also serious edge diffraction. As one reasonable criterion for practical design, we might adapt the diameter of the focusing lens to πw_p, where w_p is the pump spot size of the Gaussian beam at the focusing lens. The waist and waist location for a Gaussian beam after passing through a thin lens of focal length f can be calculated with the ABCD Matrix method. For a collimated beam with radius $w_{p'}$ they can be respectively described as

$$w_{p0} = w_p \frac{f / z'_p}{\sqrt{1 + (f / z'_p)^2}} \tag{37.a}$$

$$z'_0 = \frac{f}{f^2 / z'^2_p + 1} \tag{37.b}$$

where $z'_p = n\pi w_p^2 / M^2 \lambda_p$ is the Rayleigh range of the incoming beam. In these two equations, for simplicity, $z=0$ is considered the location of the lens. If we assume $z'_p \gg f$, which is usually satisfied for fiber-coupled end-pumped lasers, Eq. (37) are reduced to:

$$w_{po} = \frac{f \lambda_p M^2}{n\pi w_p} \tag{38.a}$$

$$z'_0 = f \tag{38.b}$$

From Eqs. (33) and (38.a) we obtain

$$F_{opt} = w_p \sqrt{\frac{g(L)}{\beta}} \tag{39}$$

where $F_{opt}=af_{opt}$ is dimensionless optimal focal length of the focusing lens is plotted in Fig. 3 as a function of L for $w_p=1$ and several pump beam quality factors β. At a fixed β, optimal focal length of the focusing lens is an increasing function of L and is not very sensitive to L when pump beam quality is poor. It can be also seen, for a specific active medium, when pump beam quality increases by increasing divergence angle and/or core diameter of the fiber a lens with a small focal length satisfies in Eq. (39) is needed to achieve an optimal focusing and consequently a higher mode-matching efficiency. At a fixed l and β, if absorption coefficient α increases the optimal focal length decreases because of the moving pump beam waist location closer to the incident surface of the active medium. Putting the values of β, L and w_p into (30) and (39), optimal focal length lens and optimal location of the focusing lens can be determined.
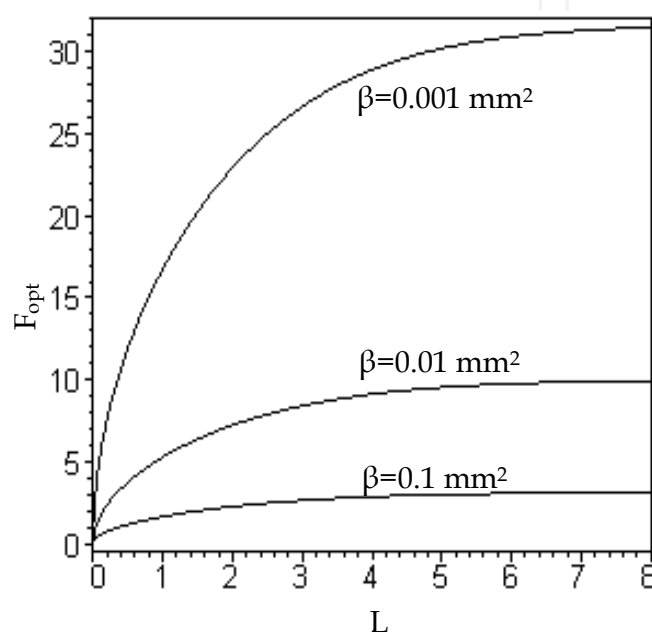
Fig. 3. Dimensionless optimized focal length of the focusing lens, $af_{opt.}$, as a function of L for $\omega_p=1$ and several pump beam quality factors β.

On the other hand, based on the paraxial approximation, pump spot size $w_p(z)$ may be given by (Fan &. Sanchez, 1990)

$$w_p(z) = w_{p0} + \theta_p |z - z_0| \tag{40}$$

Several authors (Fan & Sanchez, 1990; Laporta & Brussard, 1991; Chen, 1999; Chen et al., 1996, 1997) have considered Eq. (40) to describe the evolution of pump beam radius within the gain medium in their model. This functional dependence is appropriate for beams with partial-spatial coherence (Fan & Sanchez, 1990). Also, if one is focusing the beam to a small spot size, the paraxial approximation is not justified and making questionable using Eq. (40) which is derived under the paraxial approximation. Using this function to describe the evolution of pump beam radius, the optimum pump spot size is defined as (Chen, 1999):

$$w_{p,opt} = 2\sqrt{\beta\left[ln\left(\frac{2}{1+\exp(-L)}\right)\coth\left(\frac{L}{2}\right) - \frac{L}{\exp(L)-1} \right]} \tag{41}$$

For L≫1, this equation yields (Chen et al., 1997)

$$w_{p,opt} = 2\sqrt{\beta ln(2)} \tag{42}$$

Fig. (4) shows comparison of the optimum pump spot size using Eqs. (34) and (41). It can be seen, at a fixed β, minimum pump size is an increasing function of L. For the case of poor pump beam quality, it initially increases rapidly and then this trend becomes saturate and is not significantly sensitive to L, while for the case of a good pump beam quality, it varies smoothly with increasing L. Further, for a specific active medium with a defined L, a poorer pump beam quality leads to a higher $w_{p,opt}$ to maximize the mode matching because of governing focusability with beam quality. Note that a good agreement between the Chen's model (Chen, 1999) and present model is obtained only when the pump beam has a good quality and the deviation increases with increasing pump beam quality β.
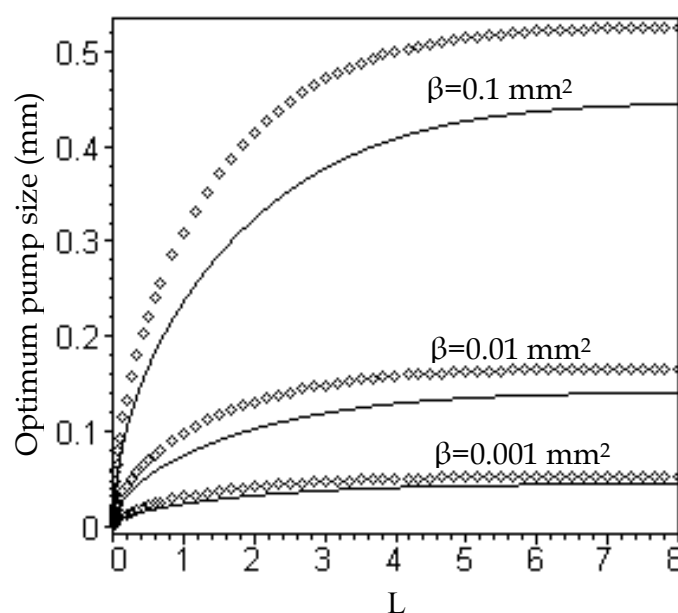
Fig. 4. Comparsion of optimum pump spot size, $w_{p,opt}$, as a function of L for values of β=0.1 and β=0.01 mm². Solid and pointed curves are calculated from Eqs. (36) and (43), respectively.

The saturation of the minimum pump spot size and hence the optimum mode-matching efficiency is due to the limit of interaction length which causes by the finite overlap distance of the beams in space. When crystal length becomes larger than the beams-overlap length in the crystal, an increasing in crystal length no larger contributing to generate the laser. To achieve the maximum mode-matching efficiency for a given crystal length and a pump beam M² factor, when absorption coefficient increases the optimum pump size should decrease. Hence, in the case of poor pump beam quality, the mode-overlapping could not be maintained through the length of the crystal and slow saturation prevented us from using a short crystal with a high absorption coefficient to improve the overlap.

To examine the accuracy of the present model, we compared Eq. (34) with the results determined by Laporta and Brussard (Laporta and Brussard, 1991). They have found that the average pump size

$$\bar{w}_p = \left[\frac{1}{l'} \int_0^{l'} w_p^2(z) dz \right]^{1/2} \tag{43}$$

with $l' = (-2.3\theta_p + 1.8)(1/\alpha)$ for $\theta_p \le 0.2$ rad or $\alpha l' \le 1.34$ can give a fairly accurate estimate of the overlap integral. l' is the effective length related to the absorption length $1/\alpha$ of the pump radiation and the divergence angle θ_p of the pump beam inside the crystal.

Fig. 5 shows a comparison of the minimum average pump size within the active medium using. Eqs. (34) and (41)-(43). It can be seen that the results calculated from (34) are in a good agreement with the results evaluated by Laporta and Brussard. Again, it can be also seen that, the optimum pump spot size in the active medium is an increasing function of β.
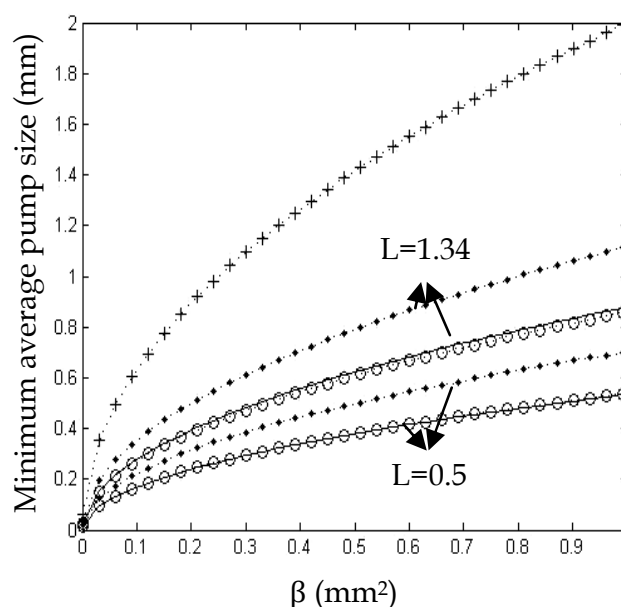
Fig. 5. Minimum pump spot size as a function of pump beam quality β for L=1.34 and L=0.5. Solid, solid diamond, open circle, and plus curves is calculated from Eqs. (34), (41), (42) and (43), respectively.

4. Optimum laser resonator

According to Eqs. (23)-(26) and (10), the output power at the condition of optimum pumping is given by

$$P_{out} = \frac{T\eta_p}{\delta} \frac{\omega_{l0}^2(\omega_{l0}^2 + 4\beta g(L))}{(\omega_{l0}^2 + 2\beta g(L))^2} \left[P_{in} - \frac{\pi\delta I_{sat}}{2\eta_p}(\omega_{l0}^2 + 2\beta g(L)) \right] \tag{44}$$

Now, we define, for generality, the normalized output efficiency as

$$\sigma_{out} = \left(\frac{P_{out}}{P_{in}} \right) \bigg/ \left(\frac{T\eta_p}{\delta} \right) = \frac{w_{l0}^2(w_{l0}^2 + 4\beta g(L))}{(w_{l0}^2 + 2\beta g(L))^2} \left[1 - \frac{(w_{l0}^2 + 2\beta g(L))}{\chi} \right] \tag{45}$$

where the input power is normalized as

$$\chi = \frac{p_{in}}{(\pi \delta I_{sat} / 2\eta_p)} \qquad (46)$$

It is often quoted in square millimeter. At a fixed β and P_{in}, the optimum mode size, $w_{l0,opt}$ for the maximum output power can be obtained by using the condition

$$\partial P_{out} / \partial w_{l0} = 0 \qquad (47)$$

This equation yields the solution

$$w_{l0,opt} = \sqrt{2\beta g(L)[h_+(\chi,\beta,L) - h_-(\chi,\beta,L) - 1]} \qquad (48)$$

where

$$h_\pm(\chi,\beta,L) = \left[\frac{\sqrt{3}\sqrt{27(\chi/2\beta g(L))^2 + 1}}{9} \pm \frac{\chi}{2\beta g(L)} \right]^{1/3} \qquad (49)$$

Fig. 6 shows a plot of optimum mode size, $w_{l0,opt}$ as a function of dimensionless crystal length, L, for several values of χ and β. One sees, at a fixed χ and β, $w_{l0,opt}$ is initially a rapidly increasing function of L, and then its dependence on L becomes weak. Also, at a fixed L, the poorer pump beam quality and larger χ leads to a larger mode size to reach a higher slope efficiency and a lower pump threshold. Increasing optimum mode size with increasing pump beam quality is attributed to the increasing optimum pump beam spot size with increasing its beam quality and maintaining the optimum mode-matching.
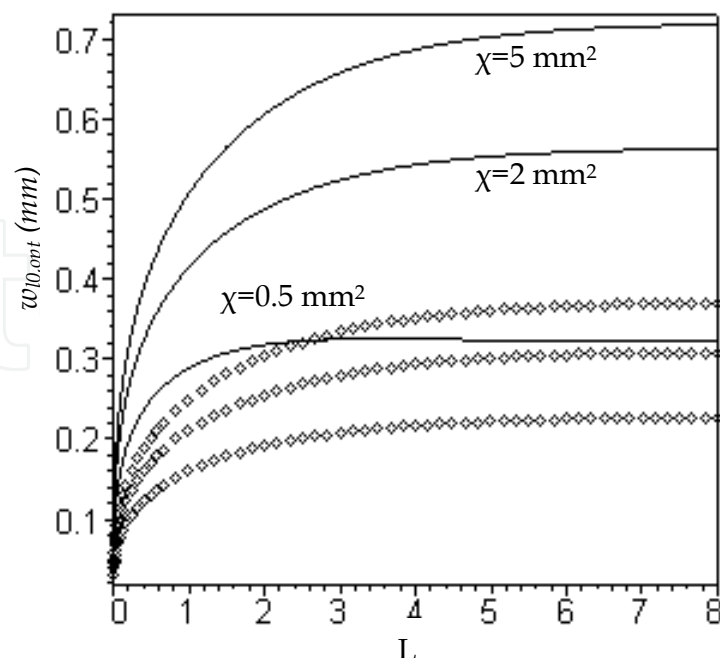

Fig. 6. Optimum mode size, $w_{l0,opt}$, as a function of dimensionless active medium length, L, for several values of χ and β. Pointed lines are for β=0.01 mm2 and solid lines are for β=0.1 mm2.

Equation (35) can be used as a guideline to design the laser resonator. First, the value of parameter β is calculated by considering values of C, n, and α. Then, for a given P_{in} and gain medium, the value of χ is determined from Eq. (46). Putting β, L and χ into (48), the optimum mode size can be determined and subsequently substituting calculated optimum mode size into (45), the maximum output efficiency $σ_{out,max}$ can be also determined.

Fig.7 shows the maximum output efficiency as a function of L for several values of χ and β. It is clear, the maximum output efficiency rapidly decreases with increasing L particularly when the available input power is not sufficiently large and beam quality is poor. It results because of the spatial-mismatch of the pump and laser beam with increasing L. Further, the influence of dimensionless gain medium length is reduced for high input power and better pump beam quality. For a poor pump beam quality, the maximum attainable output power strongly depends on the input power. This can be readily understood in the following way: the increasing pump power leads to increase the gain linearly while the better pump beam quality leads to the better pump and signal beams overlapping regardless of the value of the gain which continues to increase with increasing pump power. The large overlapping of the pump and signal beams in the crystal ensures a more efficient interaction and higher output efficiency. Note that the laser pump power limited by the damage threshold of the crystal, then χ can be an important consideration in the choice of a medium. It looks like, in the case of high pump power, the pump beam quality is a significant factor limiting to scale end-pumped solid state lasers.
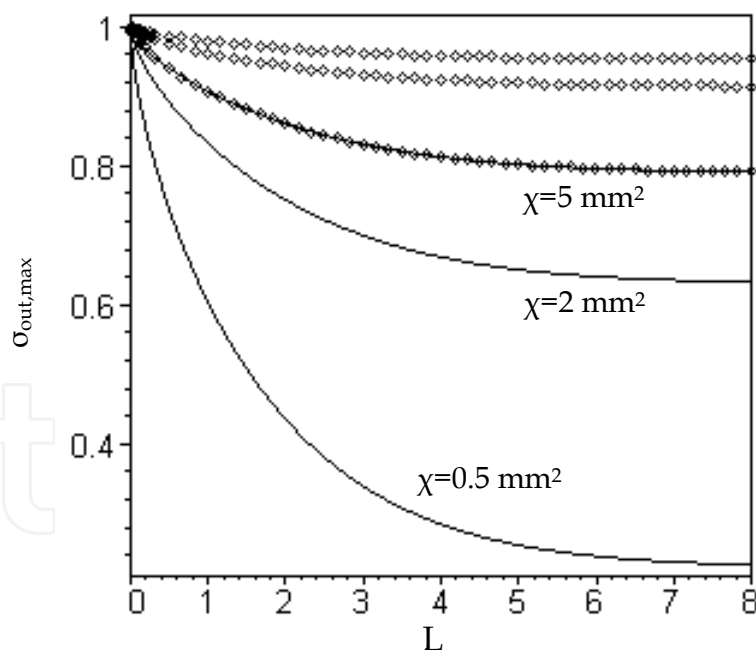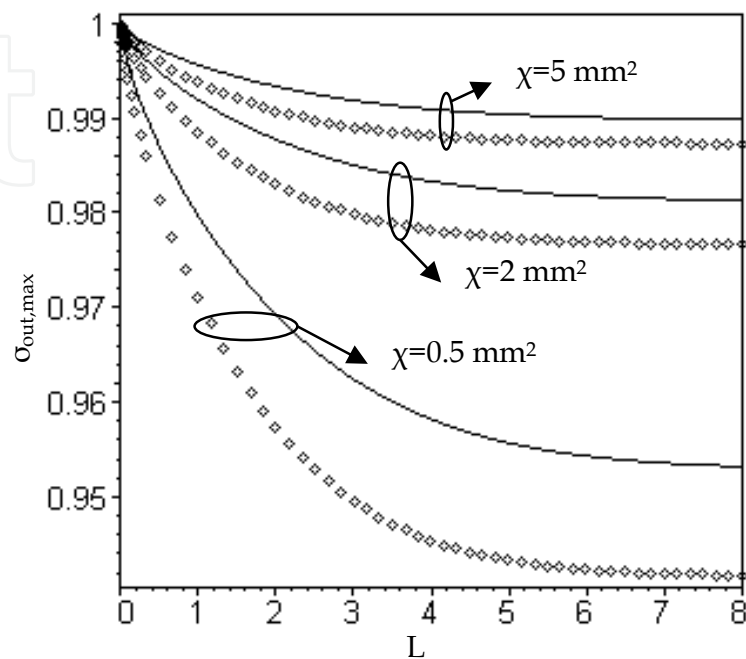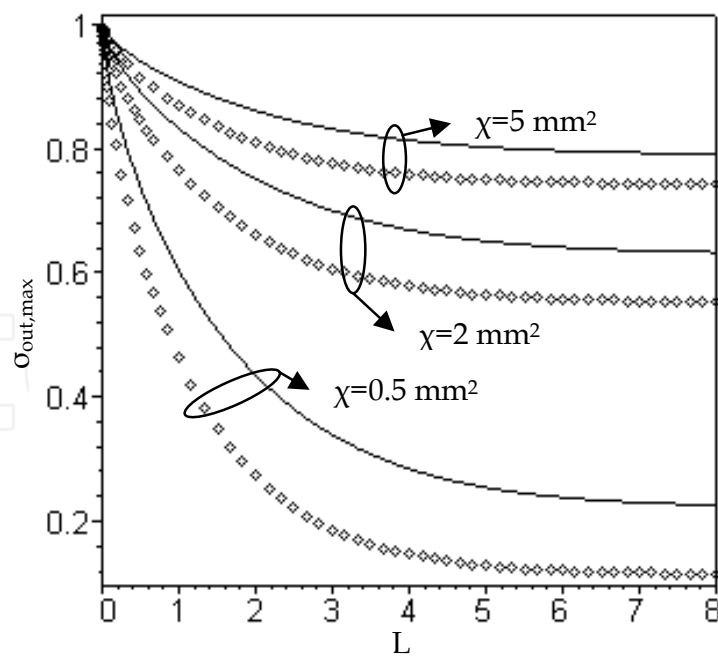

Fig. 7. Maximum output efficiency, $σ_{out,max}$, as a function of dimensionless active medium length, L, for several values of χ and β. Pointed and solid curves are for β=0.01 mm² and β=0.1mm², respectively.

In comparison, Fig. 8 shows the maximum output efficiency calculated from Eq. (45), and determined by Chen (Chen, 1999). One sees the Chen's model make a difference compared to the present model. The difference increases for low input power χ and poor pump beam

quality with increasing L. The present model shows a higher output efficiency in each value of β, χ and L. Typically, the maximum output efficiency calculated using this model is ~5%, 16%, 12% and 15% higher than those obtained from the Chen's model for sets of (L=8, χ=0.5 mm², β=0.001 mm²), (L=8, χ=0.5 mm², β=0.1 mm²), (L=1, χ=0.5 mm², β=0.1 mm²) and (L=5, χ=0.5 mm², β=0.1 mm²), respectively.

(a)

(b)

Fig. 8. Comparison of the maximum output efficiency, $\sigma_{out,max}$, as a function of L for several values of χ and (a) β=0.001 mm², (b) β=0.1 mm². Solid curves calculated from Eq. (45) and pointed curves are determined from Chen's model (Chen, 1999).

Note that we assumed the pump beam distribution comes out from the fiber-coupled laser-diodes is a Gaussian profile. Nevertheless, a more practical distribution for the output beam from the fiber-coupled laser-diodes may be closer to a Top-Hat or super-Gaussian distribution:

$$r_p(x,y,z) = \frac{\alpha}{\pi \varpi_p^2(z)[1-\exp(-\alpha l)]} \Theta(\varpi_p - \sqrt{x^2+y^2})\exp(-\alpha z) \tag{50}$$

where $\Theta(\varpi_p - \sqrt{x^2+y^2})$ is the Heaviside step function and ϖ_p is the average pump-beam radius inside the gain medium. Solving Eqs. (7) and (11) with considering (50) we can obtain mode-match-efficiency as follow:

$$F(\omega_{l0},\varpi_p) = \frac{\omega_{l0}^2}{2\varpi_p^2}\left[1-\exp\left(-2\frac{\varpi_p^2}{\omega_{l0}^2}\right)\right] \tag{51}$$

Fig. 9 shows the mode-match-efficiency calculated from (51) and (26) versus $w_{l0}/w_{p,opt}$. One sees the differences is small, especially for $w_{l0}/w_{p,opt}<1$. Therefore the Gaussian distribution can be considered a reasonable approximation for analysis the optical pump conditions.
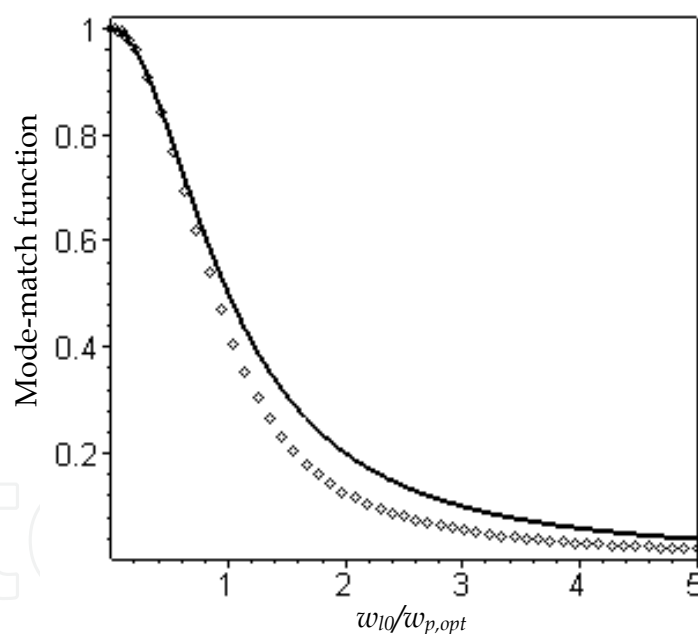

Fig. 9. Mode-match efficiency as a function of $w_{l0}/w_{p,opt}$. Solid and pointed curves represent the results for Gaussian distribution and Top-Hat profile, respectively.

5. Pump source requirements

In an end-pumped laser, the brightness of the pump source may be a critical factor for optimizing the laser performance. For instance, tight focusing of the pump beam is required to enhance the nonlinear effect for mode-locking of a femtosecond laser while the long collimation of a tight-focused pump beam is crucial for mode-matching of the laser beam

along the gain medium. According to Eq. (16), the desired exponential unsaturated gain at optimal design can be determined by the optimum mode size and the optimum average pump beam spot size:

$$\Gamma = \frac{2P_{in}\eta_p}{\pi I_{sat}} \frac{1}{w_{l0,opt}^2 + w_{p,opt}^2} \tag{52}$$

Putting Eq. (34) into (52), the small-signal round-trip gain at the optimum condition is expressed as:

$$\Gamma = \frac{2P_{in}\eta_p}{\pi I_{sat}} \frac{1}{w_{l0,opt}^2 + 2\beta g(L)} \tag{53}$$

Note that, if the volume of pump beam stays well within the volume of the fundamental cavity mode, TEM_{00} operation with diffraction-limited beam quality is often possible. It is because of, at this condition, gain of the high-order modes is too small to balance the losses and start to oscillate. Therefore, for oscillating laser in TEM_{00}, we have

$$w_{l0,opt} \geq w_{p0,opt} \tag{54a}$$

or

$$w_{l0}^2 \geq 2\beta g(L) \tag{54b}$$

The constraint condition in (54) can be rewritten as:

$$nw_{p0}\theta_p \leq \frac{w_{l0}^2 n\alpha}{2g(L)} \tag{55}$$

The brightness of the beam in the air B can be defined as (Born & Wolf, 1999):

$$B = \frac{P_{in}}{(\pi nw_{p0}\theta_p)^2} \tag{56}$$

Substituting the constraint of (55) into (56), we find

$$B \geq 4P_{in}\frac{g^2(L)}{n^2\pi^2\alpha^2 w_{l0,opt}^2} \tag{57}$$

Now, we can obtain a relation between the required brightness of the pump beam in air, desired gain Γ, properties of the gain medium (I_{sat}, l, and n) at a given pump power P_i and pump beam quality β:

$$B \geq 4P_{in}\frac{g^2(L)}{n^2\pi^2\alpha^2}\left[\frac{2\eta_p P_{in}}{\Gamma \pi I_{sat}} - 2\beta g(L)\right]^{-2} \tag{58}$$

This is a requirement on B to achieve a gain value of Γ at a pump power P_i. If the inequality in (58) is not satisfied, the laser will not work at the design point. It can be simply shown, in

the limit case of $l=2z_R=2g(L)/\alpha$ and $\beta \rightarrow 0$, Eq. (58) reduces to that of developed by Fan and Sanchez (Fan & Sanchez, 1990):

$$B \geq \frac{1}{P_{in}} \left[\frac{\Gamma l I_{sat}}{2n\eta_p} \right]^2 \tag{59}$$

The limit of $\beta \rightarrow 0$ is justified when the M^2 factor is small and the absorption coefficient is high in which the effective interaction length is much shorter than physical length of the medium.

Notice the power scaling with maintaining operation in the TEM_{00} mode has been limited by the formation of an aberrated thermal lens within the active medium. Besides the thermal lens, the maximum incident pump power is restricted by thermal fracture of the laser crystal. Therefore, it is of primary importance for the laser design to avoid thermally induced fracture and control the thermal effects.

6. Thermal effects in end-pumped lasers

The thermal lens generated within a gain medium may hinder the power scaling of such lasers by affecting the mode size of the laser inside the resonator and reducing the overlap between the pump and cavity modes. Efficient design consideration usually is dominated by heat removal and the reduction of thermal effects for high-power solid-state lasers. In end-pumped solid-state lasers the requirement for small focusing of pump beam size leads to a very high pump deposition density and further exacerbate thermal effects such as (a) thermal lensing and aberration, (b) birefringence and depolarization caused by thermal stress, (c) fracture and damaging the laser crystal by thermal expansion which limit the power-scaling of end-pumped lasers. The thermal lens in the gain medium will act as another focusing element which should be taken into account in order to optimize the matching between the cavity and the pump beams in the gain medium.

One of the main problems encountered in end-pumped lasers is beam distortion due to the highly aberrated thermal lens, making it extremely difficult to simultaneously achieve high efficiency and good beam quality. Many methods such as low quantum defect level, double-end pumping, composite crystal and low doping concentration have been proposed to reduce the thermal effects and increase output power (Koechner, 2006). The lower doping concentration and longer length crystal decrease the thermal lens effect greatly and also are preferable for the efficient conversion.

In the case of longitudinal pumping, most of the pump energy absorbed close to the end surface of the rod. This means the gradient-index lens is strongest near the pump face and the end effect localized at this first face of the rod. Since the generated lenses are located inside the crystal and the thickness of the gain medium is very small compared the cavity length, the separation between these lenses can be neglected and the combination can be well approximated by an effective single thin lens located at the end of the laser rod with the effective thermal focal length (distance from the end of the rod to the focal point) as (Shayeganrad, 2012)

$$\frac{1}{f_{th}} = \frac{\eta_h P_{in} \xi}{2\pi k_c} \frac{\alpha}{1-e^{-\alpha l}} \int_0^l \frac{e^{-\alpha z} dz}{w_p^2(z)} \tag{60}$$

where η_h is the heat conversion coefficient resulting from fluorescence efficiency, upconversion, and quantum defect, $\xi = \dfrac{\partial n}{\partial T} + (n-1)(1+v)\alpha_T + 2C_{r,t}n^3\alpha_T$ is the-averaged thermo-optic coefficient, $\partial n/\partial T$ is the thermal-optics coefficient, α_T is the thermal expansion coefficient, $C_{r,t}$ is the photo-elastic coefficient of the material, n is refractive index of the gain medium, and v is Poisson's ratio. Note that under efficient laser operation and low-loss cavity $\eta_h = 1 - \lambda_p/\lambda_l$. Also, the factor (n-1) has to be replaced by n in the case of end-pumped resonators with a high reflectivity coating on end surface of the crystal. The first term results from the thermal dispersion, the second term is caused by the axial mechanical strain, and the third term represents the strain-induced birefringence. Though for most cases contribution of thermal stress effect is small. Further, the Gaussian pump beam leads to a much more highly aberrated thermal lens, which is a factor of two stronger on axis for the same pump spot size and pump dissipation (Fan et al., 2006).

Equation (60) cannot be solved analytically. To obtain the focal length, this equation must be solved numerically. Again, similar solving mode-matching function, an average pump spot size inside the active medium is considered. Then, we have

$$\frac{1}{f_{th}} = \frac{\eta_h P_{in} \xi}{2\pi k_c} \frac{1}{\omega_{p,opt}^2} \tag{61}$$

This function shows that when pump beam spot size increases the thermal focal length increases, while a smaller pump radius needs to achieve a lower threshold and higher slope efficiency. Most importantly, when the pump beam waist is decreased, the temperature and temperature gradient in the laser rod would be very high due to the resulting heat.

Substituting Eq. (34) into Eq. (61), we can obtain thermal focal power D_{th} as:

$$D_{th} = \frac{\eta_h P_{in} \xi}{4\pi k_c \beta g(L)} \tag{62}$$

It is clear that the focal power of the thermal lens depends on the gain medium characteristics, pump beam properties and is independent on the crystal radius. It increases directly with pump power and inversely with pump beam M^2 factor. Increasing P_{in} leads to increase the deposited heat and hence increase the themprature gradiant and D_{th}. Decreasing M^2, leads to increase focusability of the beam and hence increasing D_{th}. In addition, utilizing a material with small value of ξ, and high values of thermal conductivity k_c can help to reduce the thermal effect.

Eq. (62) has the following properties: for small values of L ($L \ll 1$):

$$D_{th} = \frac{\sqrt{3}\eta_h P_{in} \xi}{2\pi k_c \beta} \tag{63}$$

and for large values of L ($L \gg 1$):

$$D_{th} = \frac{\eta_h P_{in} \xi}{4\pi k_c \beta} \tag{64}$$

It can be seen in the asymptotic, values are independent of the active medium length.

7. References

Alfrey, A. J. (1989). Modeling of longitudinally pumped CW Ti: Sapphire laser oscillators. *IEEE J. Quant. Electron*, Vol. 25 PP. 760-765.

Berger, J., Welch, D. F., Sciferes, D.R., streifer, W. and Cross, P. (1987). High power, high efficient neodymium: yttrium aluminum garnet laser end-pumped by a laser diode array. *Appl. Phys. Lett.*, Vol. 51 PP. 1212-1214.

Bollig, C., Jacobs, C., Daniel Esser, M. J., Bernhardi, Edward H., and Bergmann, Hubertus M. von. (2010). Power and energy scaling of a diode-end-pumped Nd:YLF laser through gain optimization. *Opt. Express*, Vol. 18, PP. 13993-14003.

Born M., and Wolf E. (1999). Principles of Optics. 7th extended edition, Pergoman Press Ltd. Oxford, England.

Carkson, W. A., and Hanna,D.C. (1988). Effects of transverse mode profile on slop efficiency and relaxation oscillations in a longitudinal pumped laser. *J. Modm Opt.*, Vol. 36 PP. 483-486.

Chen, Y. F. (1999). Design Criteria for Concentration Optimization in Scaling Diode End-Pumped Lasers to High Powers: Influence of Thermal Fracture. *IEEE J. Quantum Electron.*, Vol. 35, PP. 234-239.

Chen, Y. F., Kao, C. F., and Wang, C. S. (1997). Analytical model for the design of fiber-coupled laser-diode end-pumped lasers. *IEEE J. Quantum Electron.*, Vol. 133 PP. 517-524.

Chen, Y. F., Liao, T. S., Kao, C. F., Huang, T. M., Lin, K. H., and Wang, S. C. (1996). Optimization of fiber-coupled laser-diode end-pumped lasers: influence of pump-beam quality. *IEEE J. Quantum Electron.*, Vol. 32, PP. 517-524.

Clarkson, W. A., and Hanna, D. C. (1989). Effects of transverse-mode profile on slope efficiency and relaxation oscillations in a longitudinally-pumped laser. *J. Mod. Opt.* Vol. 27 PP. 483-498.

Fan, S., Zhang, X., Wang, Q., Li, S., Ding, S., and Su, F. (2006). More precise determination of thermal lens focal length for end-pumped solid-state lasers, *Opt. Commun.* Vol. 266, PP. 620-626.

Fan, T. Y., and Byer, B. L. (1988). Diode-pumped solid-state lasers. *IEEE J. Quantum Electron.*, Vol. 24, PP. 895-942.

Fan, T. Y., and Sanchez, A. (1990). Pump source requirements for end pumped lasers. *IEEE J. Quantum Electron.*, Vol. 26 PP. 311-316.

Fan, T. Y., Sanchez, A., and Defeo, W. G. (1989). Scalable end-pumped, Diode-laser pumped lasers. *Opt. Lett.*, Vol. 14 PP. 1057-1060.

Ferguson, B., and Zhang, X. C. (2002). Materials for terahertz science and technology. *Nature Materials*, Vol. 1, PP. 26-33.

Findlay, D., and Clay, R. A. (1966). The measurement of internal losses in 4-level lasers. *Physics Letters*, Vol. 20, PP. 277-278

Gong, Lu, M., Yan, C., P., and Wang, Y. (2008) Investigations on Transverse-Mode Competition and Beam Quality Modeling in End-Pumped Lasers. *IEEE J. Quantum Electron.*, Vol. 44, PP. 1009-1019.

Guo, L., Lan, R., Liu, H., Yu, H., Zhang, H., Wang, J., Hu, D., Zhuang, S., Chen,L., Zhao,Y., Xu, X., and Wang, Z. (2010). 1319 nm and 1338 nm dual-wavelength operation of LD end-pumped Nd:YAG ceramic laser. *Opt. Express*, Vol. 18, PP. 9098–9106.

Hall, D. G. (1981). Optimum mode size criterion for low gain lasers. *Appl. Opt.*, Vol. 20 PP. 1579-1583.

Hall, D. G., Smith, R. J., and Rice, R. R. (1980). Pump size effects in Nd:YAG lasers. *Appl. Opt.*, Vol. 19 PP. 3041-3043.

Hanson, F. (1995). Improved laser performance at 946 and 473 nm from a composite Nd:$Y_3Al_5O_{12}$ rod. *Appl. Phys. Lett.* Vol. 66, PP. 3549-3551.

Hemmeti, H., and Lesh, Jr. (1994). 3.5 w Q-switch 532-nm Nd:YAG laser pumped with fiber-coupled diode lasers. *Opt. Lett.* Vol. 19 PP. 1322-1324.

Hering, P., Lay, J. P., Stry, S., (Eds). (2003). Laser in environmental and life sciences: Modern analytical method. Springer, Heidelberg-Berlin.

Koechner, W. (2006). Solid state laser engineering. Sixth Revised and Updated Edition, Springer-Verlog, Berlin.

Laporta, P., and Brussard, M. (1991). Design criteria for mode size optimization in diode pumped solid state lasers. *IEEE J. Quantum Electron.*, Vol. 27 PP. 2319-1326.

MacDonald, M. P., Graf, Th., Balmer, J. E., and Weber, H. P. (2000). Reducing thermal lensing in diode-pumped laser rods. *Opt. Commun.* Vol. 178, PP. 383-393.

Maiman, T. H. (1960). Stimulated Optical Radiation in Ruby. *Nature*, Vol. 187, PP. 493-494.

Mukhopadhyay, P. K., Ranganthan, K., George, J., Sharma, S. K. and Nathan, T. P. S. (2003). 1.6 w of TEM_{00} cw output at 1.06 μm from Nd:CNGG laser end-pumped by a fiber-coupled diode laser array. *Optics & Laser Technology*, Vol. 35 PP. 173-180.

Risk, W. P. (1988). Modeling of longitudinally pumped solid state lasers exhibiting reabsorption losses. *J. Opt. Amer. B*, Vol. 5PP. 1412-1423.

Saha, A., Ray, A., Mukhopadhyay, S., Sinha, N., Datta, P. K., and Dutta, P. K. (2006). Simultaneous multi-wavelength oscillation of Nd laser around 1.3 μm: A potential source for coherent terahertz generation. *Opt. Express* , Vol. 14, PP. 4721-4726.

Sennaroghlu, A. (Ed.). (2007). Solid atate lasers and applications. CRC Press, Taylor & Francis Group.

Shayeganrad, G. (2012). Efficient design considerations for end-pumped solid-state-lasers. Optics and laser Technology, *Optics & Laser Technology*, Vol. 44, PP. 987–994.

Shayeganrad, G., and Mashhadi, L. (2008). Efficient analytic model to optimum design laser resonator and optical coupling system of diode-end-pumped solid-state lasers: influence of gain medium length and pump beam M^2 factor. *Appl. Opt.*, Vol. 47, PP. 619-627.

Sipes, D. L. (1985). Highly efficient neodymium: yttrium aluminum garnet lasers end-pumped by a semiconductor laser array. *Appl. Phys. Lett.*, Vol. 47 PP. 74-76.

Šulc, J., Jelínková, H., Kubeček, V., Nejezchleb, K.. and Blažek, K.. (2002). Comparison of different composite Nd:YAG rods thermal properties under diode pumping. *Proc. SPIE* Vol. 4630, PP. 128-134.

Weber, R., Neuenschwander, B., Donald, M. M., Roos, M. B., and Weber, H. P. (1998). Cooling schemes for longitudinally diode laser-pumped Nd:YAG rods. *IEEE J. Quantum Electron.* Vol. 34, PP. 1046-1053.

Xiea, W., Tama, S. C., Lama, Y. L., Yanga, H., Gua, J., Zhao, G., and Tanb, W. (1999). Influence of pump beam size on laser diode end-pumped solid state lasers. *Optics & Laser Technology* Vol. 31 PP. 555-558.

Zhuo, Z., Li, T., Li, X. and Yang, H. (2007). Investigation of Nd:YVO$_4$/YVO4 composite crystal and its laser performance pumped by a fiber coupled diode laser, *Opt. Commun.* Vol. 274, PP. 176-181.
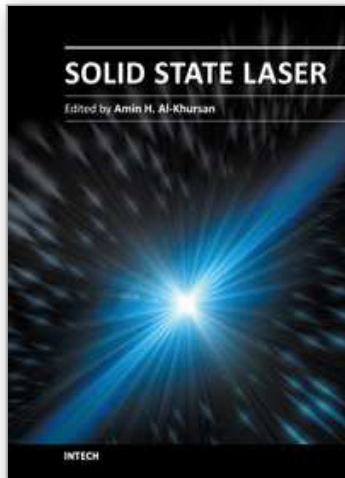
Solid State Laser

Edited by Prof. Amin Al-Khursan

This book deals with theoretical and experimental aspects of solid-state lasers, including optimum waveguide design of end pumped and diode pumped lasers. Nonlinearity, including the nonlinear conversion, up frequency conversion and chirped pulse oscillators are discussed. Some new rare-earth-doped lasers, including double borate and halide crystals, and feedback in quantum dot semiconductor nanostructures are included.

How to reference

In order to correctly reference this scholarly work, feel free to copy and paste the following:

Gholamreza Shayeganrad (2012). Optimum Design of End-Pumped Solid-State Lasers, Solid State Laser, Prof. Amin Al-Khursan (Ed.), ISBN: 978-953-51-0086-7, InTech, Available from:
http://www.intechopen.com/books/solid-state-laser/optimum-design-of-end-pumped-solid-state-lasers

INTECH
open science | open minds